II-G Biomolecular Science

Elucidation of a structure-function relationship of metalloproteins is a current subject of this group. The primary technique used for this project is the stationary and time-resolved resonance Raman spectroscopy monitored by near IR to UV lasers. The main themes that we want to explore are (1) mechanism of oxygen activation by enzymes, (2) mechanism of active proton translocation and its coupling with electron transfer, (3) coupling mechanism of proton- and electron transfers by quinones in photosynthetic reaction center, (4) higher order protein structures and their dynamics, and (5) reactions of biological NO. In category (1), we have examined a variety of terminal oxidases, cytochrome P450s, and peroxidases, and also treated their enzymatic reaction intermediates by using the mixed flow transient Raman apparatus and the Raman/absorption simultaneous measurement device. For (2) the third generation UV resonance Raman (UVRR) spectrometer was constructed and we are going to use it to the peroxy and ferryl intermediates of cytochrme c oxidase. In (3) we succeeded in observing RR spectra of quinones A and B in bacterial photosynthetic reaction centers for the first time last year, but we focused our attention on tyrosine radical this year. For (4) we developed a novel technique for UV resonance Raman measuremnts based on the combination of the first/second order dispersions of gratings and applied it successfully to 235-nm excited RR spectra of several proteins including mutant hemoglobins and myoglobins. Nowadays we can carry out time-resolved UVRR experiments with nanosecond resolution to discuss protein dynamics. We have succeeded in isolating the spectrum of β145-Tyr, β35-Tyr and α140-Tyr of Hb A separately and their changes upon quaternary structure transition. For (5) we purified soluble guanylate cyclase from bovine lung and observed its RR spectra. To understand the implication, we examined Raman spectra of NO adducts of various mutant Mbs.

II-G-1 Time-Resolved UV Resonance Raman Detection of a Transient Open Form of the Ligand Pathway in Tyr64(E7) Myoglobin

MUKAI, Masahiro[1]; NAKASHIMA, Satoru[2]; OLSON, John S.[3]; KITAGAWA, Teizo
([1]RIKEN; [2]Osaka Univ.; [3]Rice Univ.)

[*J. Phys. Chem.* **102**, 3624 (1998)]

X-ray crystallographic analyses of myoglobin (Mb) in the deoxy- and CO-bound states noted the absence of a preformed pathway for ligand movement from the heme iron to the solvent. To explore a mechanism of ligand entry, time-resolved UV resonance Raman experiments have been carried out, using a mutant with tyrosine at the distal histidine position. The results indicate the presence of a transient, open pathway which is generated after photodissociation of CO in the H64Y mutant. The Raman spectra were probed at 235 and 416 nm with a time resolution of 7 ns in the range -100 ns to 10 ms following photolysis at 532 nm. In the 235-nm excited spectra, the tyrosine bands of H64Y Mb at 1618 (Y8a) and 1176 cm^{-1} (Y9a) are noticeably intensity-enhanced shortly after photolysis but the original intensity is restored by 5 ms. The time range in which the Tyr bands are intensified is prolonged by addition of glycerol to the solvent. This intensity change is not seen with the native Mb which has three naturally occurring Tyr residues. Thus, the intensity increase observed for the mutant Mb is attributed to Tyr64. The corresponding bands of *para*-cresol derivative exhibit greater intensity in polar (H-bond forming) solvents than in nonpolar solvents. This result suggests that the increase in intensity of the Tyr bands in the transient form of the mutant myoglobin compared to that in the equilibrium form is due to exposure of Tyr64 to solvent water. Increased solvation indicates an outward movement of the phenol side chain and formation of an open channel to the distal pocket.

II-G-2 UV Resonance Raman Studies of α-Nitrosyl Hemoglobin Derivatives: Relation between the α1-β2 Subunit Interface Interactions and the Fe-Histidine Bonding of α Heme

NAGATOMO, Shigenori; NAGAI, Masako[1]; TSUNESHIGE, Antonio[2]; YONETANI, Takashi[2]; KITAGAWA, Teizo
([1]Kanazawa Univ.; [2]Univ. Pennsylvania)

[*Biochemistry* **38**, 9659 (1999)]

Human α-nitrosyl β-deoxy hemoglobin A, $\alpha^{NO}\beta^{deoxy}$, is considered to have a T(tense) structure with the low O_2 affinity extreme and the Fe-histidine(His87) (Fe-His) bond of α heme cleaved. The Fe-His bonding of α heme and the intersubunit interactions at α1-β2 contact of α^{NO}-Hbs have been examined under various conditions with EPR and UV resonance Raman (UVRR) spectra excited at 235 nm, respectively. NOHb at pH 6.7 gave the UVRR spectrum of the R structure, but in the presence of inositol-hexakis-phosphate (IHP) for which the Fe-His bond of the α heme is broken, UVRR bands of Trp residues behaved half T-like while Tyr bands remained in the R-like. The half ligated nitrosylHb, $\alpha^{NO}\beta^{deoxy}$, in the presence of IHP at pH 5.6, gave T-like UVRR spectra for both Tyr and Trp, but binding of CO to its β heme ($\alpha^{NO}\beta^{CO}$) changed the UVRR spectrum to half T-like. Binding of NO to its β heme (NOHb) changed the UVRR spectrum to 70% T-type for Trp but almost R-type for Tyr. When pH was raised to 8.2 in the presence of IHP, the UVRR spectrum of NOHb was the same as that of COHb. EPR spectra of these Hbs indicated that the Fe-His bond of α^{NO} heme is partially cleaved. On the other hand, the UVRR spectra of $\alpha^{NO}\beta^{deoxy}$ in the absence of IHP at pH 8.8 showed the T-like UVRR spectrum but EPR spectrum indicated that 40-50% of the Fe-His bond of α hemes was intact. Therefore, it became evident that there is qualitative correlation between the cleavage of the Fe-His bond of α heme and T-like contact of Trp-β37. We note that the

behaviors of Tyr and Trp residues at the α1-β2 interface are not synchronous. It is likely that the behaviors of Tyr residues are controlled by the ligation of β heme through His-β92(F8) → Val-β98(FG5) → Asp-β99(G1) → Tyr-α42(C7) or Tyr-β145(HC2).

II-G-3 Observation of Cu-N_3^- Stretching and N_3^- Asymmetric Stretching Bands for *mono*-Azide Adduct of *Rhus vernicifera* Laccase

HIROTA, Shun[1]; MATSUMOTO, Hiroki[1]; HUANG, Hong-Wei; SAKURAI, Takeshi; KITAGAWA, Teizo; YAMAUCHI, Osamu[1]
([1]Nagoya Univ.)

[*Biochem. Biophys. Res. Commun.* **243**, 435 (1998)]

Mono-azide adduct of *Rhus vernicifera* laccase, a multicopper oxidase containing one type-1 (blue) copper, one type-2 (non-blue normal) copper, and a pair of type-3 (binuclear and EPR silent) coppers, of which type-2 and type-3 coppers constitute a trinuclear site, was investigated with resonance Raman (RR) and Fourier transform infrared (FT-IR) spectroscopies as a step toward elucidation of the structure and function of the trinuclear site. The Cu-N_3^- stretching ($\nu_{Cu\text{-}N_3^-}$) RR band was observed for azide-bound multicopper oxidases for the first time. The $\nu_{Cu\text{-}N_3^-}$ band was located at 400 cm^{-1} for mono-$^{14}N_3^-$ laccase, which shifted to 396 cm^{-1} with the $^{15}N^{14}N^{14}N_3^-$ analog. The N_3^- asymmetric stretching ($\nu_{(N_3^-)asym}$) band was observed by FT-IR spectroscopy at 2035 cm^{-1} for mono-$^{14}N^{3-}$ laccase and at 2025 cm^{-1} for the $^{15}N^{14}N^{14}N_3^-$ analog. The $\nu_{Cu\text{-}N_3^-}$ and $\nu_{(N_3^-)asym}$ frequencies and their $^{15}N^{14}N$-$^{14}N^-$ isotope shifts for azido laccase correspond well with those of metazido hemocyanin, indicating that both derivatives should have a similar binding geometry of azide.

II-G-4 Studies of Bovine Enterovirus Structure by Ultraviolet Resonance Raman Spectroscopy

KAMINAKA, Shouji[1]; IMAMURA, Yoshihiro[1]; SHINGU, Masahisa[1]; KITAGAWA, Teizo; TOYODA, Tetsuya[1]
([1]Kurume Univ.)

[*J. Virol. Methods* **77**, 117 (1999)]

The structural comparison of bovine enterovirus MZ468 strain before and after the heat treatment was studied by ultraviolet resonance Raman (UVRR) spectra excited at both 235 and 251 nm. The difference between full, heated full and purified empty particles, which were expected as an in vitro model of uncoating, were demonstrated. At 235 nm excitation, the Raman bands of the capsid protein dominated in all the UVRR spectra. The UVRR spectra of the empty particles exhibited non-homogenious broadening for tryptophan W3 band and W7 Fermi doublet bands, which were characteristics of hydrophobic environment, when compared with those of the full particles. The results indicates that some Trp indole rings of the full particles were packaged inside the viral capsids and not strained by virion assembly. On the other hand, the Raman bands assigned to guanine residues of the single stranded-RNA genome were enhanced strongly in the 251-nm excited UVRR spectrum. The spectral differences between the packaged (full particles) and the unpackaged virions (heated full particles) indicates that some guanine residues had strong hydrogen bonds in the full particles.

II-G-5 Spectroscopic Characterization and Kinetic Studies of a Novel Plastocyanin from the Green Alga *Ulva pertusa*

SASAKAWA, Yuki[1]; ONODERA, Kazuhiko[1]; KARASAWA, Machiko[1]; IM, Sang-Choul[1]; SUZUKI, Eiji[1]; YOSHIZAKI, Fuminori[2]; SUGIMURA, Yasutomo[2]; SHIBATA, Naoki[3]; INOUE, Tsuyoshi[3]; KAI, Yasushi[3]; NAGATOMO, Shigenori; KITAGAWA, Teizo; KOHZUMA, Takamitsu[1]
([1]Ibaraki Univ.; [2]Toho Univ.; [3]Osaka Univ.)

[*Inorg. Chim. Acta* **283**, 184 (1998)]

A novel plastocyanin from the green alga *Ulva pertusa* was isolated and characterized. The electronic absorption and the electron paramagnetic resonance spectroscopic properties of *Ulva* plastocyanin showed features characteristic of the usual plastocyanins reported so far. However, the resonance Raman spectrum on excitation at 607 um indicated the Raman band of Cu-S_{cys} at 413 cm^{-1}; this is at a lower frequency than the corresponding Raman band of higher plant plastocyanins. Electron-transfer reactions were investigated with $[Fe(CN)_6]^{3-}$ and $[Co(phen)_3]^{3+}$ complexes. The electron-transfer rate constant of *Ulva* plastocyanin was determined to be $(1.18 \pm 0.06) \times 10^5$ $M^{-1}s^{-1}$ for the reaction with $[Fe(CN)_6]^{3-}$ at pH 7.5, and the intramolecular electron-transfer rate constant and equilibrium constant for complex formation for the reaction with $[Co(phen)_3]^{3+}$ were evaluated to be 7.7 ± 0.6 s^{-1} and $(4.2 \pm 0.4) \times 10^2$ M^{-1} respectively. The electron-transfer rate constant for the reaction with $[Fe(CN)_6]^{3-}$ at pH 7.5 is two times larger than the values obtained from the other higher plant plastocyanins. The kinetic behavior suggested that the structure is slightly different from those of other plastocyanins. It has been reported that the electron-transfer reaction of plastocyanin is inhibited by the protonation of the active site histidine (His87 in poplar plastocyanin) at acidic pH. The dependence on pH of the rate constant for the reaction with $[Fe(CN)_6]^{3-}$ was investigated. The acid-dissociation constant accompanying the electron-transfer reaction was determined to be $pK_H = 5.8$. Second-order rate constants for the reduction of plastocyanin by cytochrome c were determined to be $(1.71 \pm 0.04) \times 10^6$ $M^{-1}s^{-1}$ at $I = 0.1$ M (NaCl), pH 7.0 (20 mM Tris-HCl buffer). The saturation kinetic behavior for the reaction was not observed even at the lower ionic strength (20 mM Tris-HCl).

II-G-6 Aliphatic Hydroxylation by a Bis(μ-Oxo)-Dinickel(III) Complex

ITOH, Shinobu[1]; BANDOH, Hideki[1]; NAGATOMO, Shigenori; KITAGAWA, Teizo; FUKUZUMI, Shunichi[1]

([1]Osaka Univ.)

[*J. Chem. Soc.* in press]

Treatment of $[(\mathbf{L}^{X}Ni^{II})_2(\mu\text{-}OH)_2]^{2+}$ ($\mathbf{L}^{X}$ = *p*-substituted *N*,*N*-bis[2-(2-pyridyl)ethyl]-2-phenylethylamine; X = OMe, Me, H, Cl) with one equivalent of H_2O_2 gave a bis(μ-oxo)dinickel(III) complex, $[(\mathbf{L}^{X}Ni^{III})_2(\mu\text{-}O)_2]^{2+}$, the formation of which has been confirmed by a characteristic absorption band at 408 nm (ε = 6000 $M^{-1}cm^{-1}$) and a resonance Raman band at 612 cm^{-1} that shifts to 580 cm^{-1} upon ^{18}O-substitution. The bis(μ-oxo)-dinickel(III) complex gradually decomposes to lead to benzylic hydroxylation of the ligand side arm (phenethyl group). Rates of the formation and decay of the bis(μ-oxo)dinickel(III) complex were determined directly by monitoring the absorption change at 408 nm at low temperatures. The kinetic data of the ligand hydroxylation process including kinetic deuterium isotope effect (KIE), p-substituent effects (Hammett plot), and activation parameters ($\Delta H^{\neq}$ and $\Delta S^{\neq}$) have indicated that the bis(μ-oxo)dinickel(III) complex behaves as an electrophilic radical as in the case of bis-(μ-oxo)dicopper(III) complexes.

II-G-7 The Structure and Unusual pH Dependence of Plastocyanin from the Fern Dryopteris Crassirhizoma: The Protonation of an Active Site Histidine is Hindered by π-π Interactions

KOHZUMA, Takamitsu[1]; INOUE, Tsuyoshi[2]; YOSHIZAKI, Fuminori[3]; SASAKAWA, Yuki[1]; ONODERA, Kazuhiko[1]; NAGATOMO, Shigenori; KITAGAWA, Teizo; UZAWA, Sachiko[3]; ISOBE, Yoshiaki[3]; SUGIMURA, Yasutomo[3]; GOTOWDA, Masaharu[2]; KAI, Yasushi[2]
([1]Ibaraki Univ.; [2]Osaka Univ.; [3]Toho Univ.)

[*J. Biol. Chem.* **274**, 11817 (1999)]

Spectroscopic properties, amino acid sequence, electron transfer kinetics, and crystal structures of the oxidized (at 1.7 Å resolution) and reduced form (at 1.8 Å resolution) of a novel plastocyanin from the fern *Dryopteris crassirhizoma* are presented. Kinetic studies show that the reduced form of *Dryopteris* plastocyanin remains redox-active at low pH under conditions where the oxidation of the reduced form of other plastocyanins is inhibited by the protonation of a solvent-exposed active site residue, His87 (equivalent to His90 in *Dryopteris* plastocyanin). The x-ray crystal structure analysis of *Dryopteris* plastocyanin reveals π-π stacking between Phe12 and His90, suggesting that the active site is uniquely protected against inactivation. Like higher plant plastocyanins, *Dryopteris* plastocyanin has an acidic patch, but this patch is located closer to the solvent-exposed active site His residue, and the total number of acidic residues is smaller. In the reactions of *Dryopteris* plastocyanin with inorganic redox reagents, the acidic patch (the "remote" site) and the hydrophobic patch surrounding His90 (the "adjacent" site) are equally efficient for electron transfer. These results indicate the significance of the lack of protonation at the active site of *Dryopteris* plastocyanin, the equivalence of the two electron transfer sites in this protein, and a possibility of obtaining a novel insight into the photosynthetic electron transfer system of the first vascular plant fern, including its molecular evolutionary aspects. This is the first report on the characterization of plastocyanin and the first three-dimensional protein structure from fern plant.

II-G-8 Model Complexes of the Active Form of Galactose Oxidase. Physicochemical Properties and Reactivity of Cu(II)- and Zn(II)- Phenoxyl Radical Complexes of the Novel Organic Cofactor

ITOH, Shinobu[1]; TAKI, Masayasu[1]; KUMEI, Hideyuki[1]; TAKAYAMA, Shigehisa[1]; NAGATOMO, Shigenori; KITAGAWA, Teizo; SAKURADA, Norio[2]; ARAKAWA, Ryuichi[2]; FUKUZUMI, Shunichi[1]
([1]Osaka Univ.; [2]Kansai Univ.)

[*Angew. Chem., Int. Ed. Engl.* in press]

Model complexes of the active sites of galactose oxidase (GAO) and glyoxal oxidase (GLO) have been prepared using new cofactor models, 2-methylthio-4-*tert*-butyl-6-[[bis[2-(2-pyridyl)ethyl]amino]methyl]-phenol (**1H**) and 2,4-di-*tert*-butyl-6-[[bis[2-(2-pyridyl)-ethyl]amino]methyl]phenol (**2H**). Deprotonated ligand $\mathbf{1}^{-}$ forms dimeric Cu(II)-and Zn(II)-complexes, $[Cu^{II}_2(\mathbf{1}^{-})_2](PF_6)_2$ and $[Zn^{II}_2(\mathbf{1}^{-})_2](PF_6)_2$, in the solid state, but those complexes were converted into the monomers, $[Cu^{II}(\mathbf{1}^{-})(AcO^{-})]$ and $[Zn^{II}(\mathbf{1}^{-})(CH_3CN)]^{+}$, in solution by the coordination of acetate ion and CH_3CN, respectively. On the other hand, $\mathbf{2}^{-}$ forms monomeric Cu(II)- and Zn(II)-complexes, $[Cu^{II}(\mathbf{2}^{-})(CH_3CN)]PF_6$ and $[Zn^{II}(\mathbf{2}^{-})(CH_3CN)]PF_6$, both in the solid state and in solution. The structures and the physical properties of the Cu(II)- and the Zn(II)-complexes of the phenolate derivatives ($\mathbf{1}^{-}$ and $\mathbf{2}^{-}$) have been explored as the models for the resting sate of the enzymes. Oxidation of the Cu(II)- and Zn(II)-complexes of $\mathbf{1}^{-}$ and $\mathbf{2}^{-}$ by $(NH_4)_2[Ce^{IV}(NO_3)_6]$ (CAN) affords the corresponding phenoxyl radical complexes, $[M^{II}(\mathbf{1}^{\bullet})(NO_3^{-})]^{+}$ and $[M^{II}(\mathbf{2}^{\bullet})(NO_3^{-})]^{+}$ (M = Cu and Zn), the electronic structures and the physicochemical properties of which have been examined by UV-vis, resonance Raman, ESI-MS, and ESR. The radical complexes $[M^{II}(\mathbf{1}^{\bullet})(NO_3^{-})]^{+}$ are relatively stable at ambient temperature to show very broad absorption bands in the long wavelength region (λ_{max} = 867 and 887 nm for Cu(II)- and Zn(II)-complexes, respectively) as observed for the *active form* of the native enzymes. The Cu(II)-phenoxyl radical complexes oxidize benzyl alcohol derivatives to benzaldehydes quantitatively via a formal $2e^{-}/2H^{+}$ mechanism, where the Cu(II)-phenoxyl radical complexes are converted into the corresponding Cu(I)-phenol complexes. On the other hand, oxidation of benzyl alcohols by the Zn(II)-phenoxyl radical complexes requires two equivalents of the radical complex per alcohol, indicating that the redox reaction takes place only at the phenoxyl radical site in a dimeric form. Such a difference in the reactivity between the

Cu(II)- and the Zn(II)-complexes clearly demonstrates the importance of the redox cycle between Cu(I) and Cu(II) as well as the interconversion between the phenol and phenoxyl radical froms for the efficient two-electron oxidation of alcohols at the *mononuclear copper site* of GAO. Substituent effects of the thioether group on the reactivity are also discussed in relation with the physicochemical properties of the Cu(II)- and Zn(II)-phenoxyl radical complexes.

II-G-9 A Bis(μ-Oxo)Dicopper(III) Complex with Sterically Hindered Aromatic Nitrogen Donors: Structural Characterization and Reversible Conversion between Copper(I) and Bis(μ-Oxo)-Dicopper(III) Species

HAYASHI, Hideki[1]; FUJINAMI, Shuhei[1]; NAGATOMO, Shigenori; OGO, Seiji; SUZUKI, Masatatsu[1]; UEHARA, Akira[1]; WATANABE, Yoshihito; KITAGAWA, Teizo
([1]Kanazawa Univ.)

[*J. Am. Chem. Soc.* in press]

Recently, Tolman *et al.* and Stack *et al.* have prepared high-valent $Cu(III)_2(\mu\text{-}O)_2$ species generated by the O-O bond scission of O_2^{2-}- which exhibited monooxygenase activity. Crystallographically characterized bis(μ-oxo)dicopper(III) complexes reported so far consist of tridentate or bidentate aliphatic nitrogen donors. It is important to explore how the nature of donor atoms and the stereochemistry of ligands influence the structures and properties of bis(μ-oxo)-dicopper(III) complexes. In this context, we have synthesized a bis(μ-oxo)dicopper(III) complex, $[Cu_2(O)_2(Me_2\text{-tpa})_2](PF_6)_2\cdot 2(CH_3)_2CO$ (**1b**), having a tetradentate tripodal ligand containing aromatic nitrogen donors. Complex **1b** is the first crystallographically characterized bis(μ-oxo)dicopper(III)) complex having

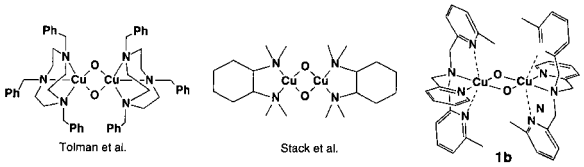

aromatic nitrogen donors.

The most striking feature of **1b** is the reversible conversion with a precursor copper (I) complex $[Cu(Me_2\text{-tpa})]^+$ (**1a**) in CH_2C1_2 at –80 °C by bubbling N_2 gas. Such reversible behavior has not been observed for the bis(μ-oxo)dicopper(III) complexes. Complex **1b** exhibited monooxygenase activity for the Me_2-tpa ligand to produce a N-dealkylated product, (6-methyl-2-pyridylmethyl)(2-pyridylmethyl)amine together with 6-methylpyridine-2-carbaldehyde in which oxygen atom comes from dioxygen. The results indicate that N-dealkylation appears to proceed through oxygen atom transfer from the bridging oxo group to the methylene carbon atom of the 6-methyl-2-pyridylmethyl side arm.

II-H Fast Dynamics of Photoproducts in Solution Phases

Picosecond time-resolved resonance Raman (ps-TR^3) spectroscopy is a promising technique to investigate ultrafast structural changes of molecules. However, this technique has not been used as widely as nanosecond TR^3 spectroscopy, mainly due to the lack of light source which has suitable repetition rates of pulses and wavelength tunability. In order to obtain qualified TR^3 spectra, first we need two independently tunable light sources for pump and probe pulses. Second, the repetition rate should be higher than kilohertz to keep a moderate average laser power without allowing the photon density of probe pulse too high. We succeeded in developing light sources for ps-TR^3 spectroscopy having wide tunability and kHz repetition, and applied them to study fast dynamics of photo-excited molecules. For carbonmonoxy myoglobin (MbCO), vibrational relaxation with the time costant of 1.9 ps was observed for CO-photodissociated heme. For Ni-octaethylporphyrin in benzene, differeces in rise times of population in vibrationally excited levels among various modes were observed in the anti-Stokes spectra for the first time. For the same molecule in piperidine, coordination of two solvent molecules was observed in the transient (*d,d*) excited state. The ps-TR^3 experiments were also applied to Zn-porphyrin dimers, for which some evidence for the π-π interaction in the S_1 state was obtained. The UV ns-TR^3 experiments on MbCO demonstrated the presence of a transient open form of the ligand pathway.

II-H-1 Intramolecular Vibrational Energy Redistribution and Intermolecular Energy Transfer in the (*d,d*) Excited State of Nickel Octaethylporphyrin

MIZUTANI, Yasuhisa; UESUGI, Yuki; KITAGAWA, Teizo

[*J. Chem. Phys.* **111**, 8950 (1999)]

The formation of a vibrationally excited photoproduct of nickel octaethylporphyrin (NiOEP) upon (π,π*) excitation and its subsequent vibrational energy relaxation were monitored by picosecond time-resolved resonance Raman spectroscopy. Stokes Raman bands due to the photoproduct instantaneously appeared upon the photoexcitation. Their intensities decayed with a time constant of ~300 ps, which indicates electronic relaxation from the (*d,d*) excited state (B_{1g}) to the ground state (A_{1g}), being consistent with the results of transient absorption measurements by Holten and coworkers [D. Kim, C. Kirmaier and D. Holten, *Chem. Phys.* **75**, 305 (1983); J. Rodriguez and D. Holten, *J. Chem. Phys.* **91**, 3525 (1989)]. The Raman frequencies of NiOEP in the (*d,d*) excited state are shifted to lower frequencies compared to those of the ground state species, and it is reasonably interpreted by the core size expansion of the macrocycle by 0.05 Å upon the

electron promotion from the d_{z^2} to the $d_{x^2-y^2}$ orbital. Anti-Stokes ν_4 intensity in vibrationally excited (*d*,*d*) state of NiOEP appeared promptly and decayed with time constants of 11 ± 2 and 330 ± 40 ps. The former is ascribed to vibrational relaxation, while the latter corresponds to the electronic relaxation from the (*d*,*d*) excited state to the electronic ground state. In contrast, the rise of anti-Stokes ν_7 intensity was not instantaneous, but delayed by 2.6 ± 0.5 ps, which indicates that intramolecular vibrational energy redistribution has not been completed in subpicosecond time regime. The peak position of ν_4 band shifted by nearly 5 cm^{-1} between 0 and 50 ps. The time constant for the shift of the ν_4 band was 9.2 ± 1.3 ps, which was close to that for the fast component of intensity decay of anti-Stokes bands. The ν_4 band became narrower and symmetric as the delay time increases. These can be ascribed to intramolecular anharmonic coupling of the ν_4 mode with the low frequency modes which can exchange energy with solvent molecules. The intra- and intermolecular vibrational energy relaxation in the metal excited state will be discussed.

II-H-2 Time-Resolved Resonance Raman Study of Intermediates Generated after Photodissociation of Wild-type and Mutant CO-Myoglobins

NAKASHIMA, Satoru[1]; KITAGAWA, Teizo; OLSON, John S.[2]
([1]Osaka Univ.; [2]Rice Univ.)

[*Chem. Phys.* **228**, 323 (1998)]

Time-resolved resonance Raman (TR^3) spectroscopy was applied to elucidate transient structures of myoglobin (Mb) involved in its ligand binding. Pump/probe Raman measurements of the Fe-CO stretching bands ($\nu_{Fe\text{-}CO}$) were carried out for various delay times (Δt = –20 ns – 1 ms with a time resolution of 7 ns) after laser photolysis of native and mutant COMb complexes. His64(E7) and Leu29(B10) were replaced with an aliphatic and aromatic residues. The static $\nu_{Fe\text{-}CO}$ frequencies of the mutants depended strongly on the environments around the bound CO and correlated more with the hydropathy indices of the replaced residues than with their sizes. The kinetics of bimolecular CO recombination correlate with the static $\nu_{Fe\text{-}CO}$ frequencies; a lower frequency generally results in faster rebinding. Despite these differences, all the proteins exhibited the shift of a porphyrin band from 370 to 379 cm^{-1} upon binding of CO and also a transient Raman band at ~497 cm^{-1}, which occurred before recovery of the original $\nu_{Fe\text{-}CO}$ band. The latter frequency was unaffected by isotopically labeling the ligand with $^{13}C^{18}O$. The 497 cm^{-1} band was absent in the spectrum at Δt = 0 ns for all of the myoglobins examined except for the His64 → Leu (H64L) mutant which shows the band immediately after photolysis. The 370 and 497 cm^{-1} bands are associated with the $C_\beta C_c C_d$ in-plane bending of the propionic side chains and the out-of-plane γ_{12} containing pyrrole swiveling and propionic bending motions, respectively. The 497 cm^{-1} transient band appears to reflect a deoxyheme intermediate in which the hydrogen bonding lattice between Arg45(CD3), His64(E7), the heme-6-propionate, and an external distal pocket water molecule is temporarily disrupted. This disruption allows larger movements of the propionate side chain, explaining intensity enhancement of the 497 cm^{-1} band. Recovery of the hydrogen bonding lattice dampens the movements of the propionate $C_\beta C_c C_d$ bond system and finally fixes it in the heme plane in the CO-bound form, causing the frequency shift of the bending mode from 370 cm^{-1} back to 379 cm^{-1}. In the Leu64 mutant, the external water molecule is already absent, facilitating rapid movement of the heme-6-propionate after photolysis. Larger scale movements of all three side chains could create an open conformation with a channel from the heme iron to the solvent, allowing ligand escape and/or rebinding.

II-H-3 Characterization of Stimulated Raman Scattering of Hydrogen and Methane Gases as a Light Source of Picosecond Time-Resolved Raman Spectroscopy

UESUGI, Yuki; MIZUTANI, Yasuhisa; KRUGLIK, Sergei G.[1]; SHVEDKO, Alexander G.[1]; ORLOVICH, Valentin A.[1]; KITAGAWA, Teizo
([1]Natl. Acad. Sci. Belarus)

[*J. Raman Spectrosc.* in press]

Stimulated Raman scattering (SRS) in compressed hydrogen and methane gas has been characterized in terms of pulse energy, temporal width, and spectral width in the range of gas pressures of 10–60 atm. to use it as a light source of picosecond time-resolved resonance Raman spectroscopy. SRS was pumped by the second harmonic of a Ti:sapphire oscillator-regenerative amplifier laser system with pulse energy up to 200 μJ, duration of ~2.5 ps and repetition rate of 1 kHz. The output spectral region of 421–657 nm was covered by the first and second Stokes SRS components on tuning of the pump wavelength in the range of 375–425 nm, Energy conversion to the first Stokes SRS component was more than 10% with H_2 and more than 20% with CH_4. The temporal width of SRS-pulse (1.1–2.1 ps) was shorter than that of a pump pulse. Spectral band shape was found to be modulated, since the SRS is generated in a transient regime. When more than 100 pulses were averaged over, the temporal and spectral profiles of SRS-pulses were sufficiently smooth and energy fluctuations were sufficiently small for spectroscopic applications. On the basis of the results obtained, an optimized condition as a Raman shifter was settled. The Raman shifter served as a light source for two-color pump-probe time-resolved resonance Raman (TR^3) experiments and to demonstrate its capabilities, picosecond TR^3 spectra of nickel tetraphenylporphyrin in toluene solution have been measured.

II-H-4 Nanosecond Temperature Jump and Time-Resolved Raman Study of Thermal Unfolding of Ribonuclease A

YAMAMOTO, Kohji[1]; MIZUTANI, Yasuhisa;

KITAGAWA, Teizo
([1]GUAS)

A nanosecond temperature jump (T-jump) apparatus heating at 1.56 μm was constructed and combined with time-resolved Raman measurements to investigate thermal unfolding of a protein for the first time. The 1.56 μm-heat pulse with 9 ns width was obtained through the two-step stimulated Raman scattering in D_2 gas involving seeding and amplification excited by the fundamental (1064 nm) of a Nd:YAG laser. The energy of the heiat pulse was 135 mJ at 10 Hz repetition when the power of the 1064 nm-input was 560 mJ, and the pulse-to-pulse fluctuation was less than 10%. To achieve uniform temperature rise in the illuminated part, the counter-propagation geometry was adopted. The magnitude of temperature rise was determined by anti-Stokes to Stokes Raman intensity ratio of the 317 and 897 cm^{-1} bands of MoO_4^{2-} aqueous solution measured at various delay times with the second harmonic (532 nm) of another Nd:YAG laser. The T-jump as large as 9 °C was attained within the temporal width of the heat pulse. The thermal unfolding of bovine pancreatic ribonuclease A (RNase A) was monitored with time-resolved Raman spectroscopy following T-jump with this apparatus. In the initial 200 ns after T-jump, the C-S stretching Raman band of methionine residues exhibited 10% change of that expected from the steady state spectra and another 10% in 5 ms. The Raman intensity of SO_4^{2-} ions around 980 cm^{-1} increased and was shifted to a lower frequency than the steady state frequency of the elevated temperature at 100 μs delay, presumably due to partial release from the active site. The Raman bands of S-S stretches and tyrosine doublets displayed little change within 5 ms, although appreciable changes were expected from the steady state spectra. Thus, it has been demonstrated for the first time for proteins that the combination of laser T-jump with time-resolved Raman spectroscopy will serve as a powerful tool for studies of thermal unfolding and that the conformation change in the initial step of unfolding is not always concerted.

II-H-5 Evidence for π-π Interactions in the S_1 State of Zn Porphyrin Dimers Revealed by Picosecond Time Resolved Resonance Raman Spectroscopy

NAKASHIMA, Satoru[1]; TANIGUCHI, Seiji[1]; OKADA, Tadashi[1]; OSUKA, Atsuhiro[2]; MIZUTANI, Yasuhisa; KITAGAWA, Teizo
([1]Osaka Univ.; [2]Kyoto Univ.)

[*J. Phys. Chem. A* in press]

The S_1 states of Zn(II) porphyrin dimers have been investigated with picosecond time-resolved resonance Raman spectroscopy. The transient absorption and Raman spectra of porphyrin dimers, in which two Zn(II)-porphyrins are covalently linked at the *ortho* or *meta* positions of phenylene spacers, are compared with those of their component monomer unit. Although Q-band of the *ortho* dimer was definitely different from those of the *meta* dimer and reference monomer, the ground state Raman spectra of the *ortho* and *meta* dimers are nearly the same as that of monomer, suggesting that the porphyrin π-π interactions do appear in the excited state of the *ortho* dimer but little in the ground state. Several characteristic Raman bands were observed for the S_1 excited state at 2 ps after photo-excitation. The monomer in the S_1 state gave the marker bands at slightly lower frequencies (by 3–4 cm^{-1}) than the corresponding ground state molecules and they did not show frequency shifts with time between 2 and 300 ps. On the contrary, in the case of the *ortho* dimer, two characteristic bands (ν_2, ν_4) appeared at frequencies significantly lower (by 10–13 cm^{-1}) than the corresponding ground state bands, and in addition the frequency of ν_4 band exhibited an upshift around 10–20 ps following photoexcitation. The frequency shift of the *ortho* dimer was appreciably perturbed by steric hindrance between the two porphyrin groups introduced through bulky *tert*-butyl group at *para* position. The behaviors of transient Raman bands of the meta dimer appeared intermediate between the monomer and the *ortho* dimer. These observations give the first clear evidence for the presence of π-π interactions in the S_1 excited state of porphyrin dimers with phenylene spacer and the occurrence of relaxation toward the monomer-type structure in several tens picoseconds.